Materials Science and Engineering C 66 (2016) 119–129

Contents lists available at ScienceDirect

Materials Science and Engineering C

journal homepage: www.elsevier.com/locate/msec

The effect of simulated inflammatory conditions on the surface properties of titanium and stainless steel and their importance as biomaterials

Abril Fonseca-García [a,b], J. Pérez-Alvarez [a,*], C.C. Barrera [c], J.C. Medina [a,b], A. Almaguer-Flores [d], R. Basurto Sánchez [e], Sandra E. Rodil [a]

[a] Instituto de Investigaciones en Materiales, Universidad Nacional Autónoma de México, México
[b] Posgrado en Ciencia e Ingeniería de Materiales, Universidad Nacional Autónoma de México, México
[c] Posgrado en Ciencias Médicas, Odontológicas y de la Salud, Universidad Nacional Autónoma de México, México
[d] Facultad de Odontología, Universidad Nacional Autónoma de México, México
[e] Instituto Nacional de Investigaciones Nucleares, México

ARTICLE INFO

Article history:
Received 27 November 2015
Received in revised form 29 February 2016
Accepted 11 April 2016
Available online 16 April 2016

Keywords:
Titanium
Medical grade stainless steel
Inflammatory conditions
Surface energy
Roughness
Surface charge
Corrosion resistant

ABSTRACT

This work compares the surface modifications induced by the immersion in solutions that simulate inflammatory conditions of pure titanium (cpTi) and medical grade stainless steel (SS). The inflammatory conditions were simulated using a mixture of Hartman solution and 50 mM of hydrogen peroxide (H_2O_2) at pH = 5.2. The samples were immersed by 7 days refreshing the solution every day to keep the reactivity of the H_2O_2. The surface characteristics that were investigated were: elemental composition by X-ray photoelectron spectroscopy (XPS); topography by atomic force microscopy (AFM) and profilometry; wettability and surface energy by sessile drop contact angle and point of zero charge by titration. Moreover, the variations in the electrochemical response were evaluated by open circuit potential (OCP), electrochemical impedance spectroscopy (EIS) and potentiodynamic polarization (PP) performed before and after the treatment using the Hartman solution as the electrolyte. The XPS results indicated that for both metallic samples, oxidation of the surface was promoted and/or the oxide layer was thicker after the immersion. The roughness and the solid-liquid surface energy were increased; the samples showed a more hydrophilic character after the treatment. However, the surface energy of the solid estimated using the Van Oss–Chaudhury–Good approach showed different trends between the cpTi and the SS surfaces; the polar component decreased for cpTi, while it increased for SS. Finally, the electrochemical results indicated that the corrosion resistance (R_{cor}) and the pore resistance (R_{po}) significantly decreased for cpTi, while both resistances were not significantly different for the SS. This is indicative of a higher dissolution of the cpTi compared to SS and the lower R_{po} means that the species are easily transported through the surface layer, which can be explained in terms of the formation of a porous TiO_x layer, not observed on the SS. The cpTi surface suffered from a dissolution/oxidation process that allows its integration with the surrounding media, while the SS remained completely passive and this different response might be related to their distinguished clinical outcome.

1. Introduction

Titanium and its alloys are currently the standard metallic materials for orthopedic and dental implants due to its superior properties compared to other biocompatible metal alloys, such as medical grade stainless steel and cobalt-chrome alloys [1–3]. Titanium alloys are the only metallic materials that present osseointegration, defined as a structural and functional connection between the living bone and the implant surface [4–6]. The reason for such behavior is not completely understood yet and different models have been proposed, such as the affinity of the dielectric constant of the native titanium oxide to water, which induces low polarizability of the surface and therefore not strong electrostatic forces that could lead to the unfolding or loss of conformation of the adsorbed proteins [3]. Another model is the formation of an hydrated porous TiOOH layer during the initial period of implantation as a consequence of the interaction with reactive oxygen species produced during the inflammatory process that occurs after implantation [7]. The model proposes that the porous layer, in conjunction with the other physicochemical properties of the TiO_x surface promotes the accumulation of Ca^{2+} and phosphate ions. The initial research to investigate the interaction of titanium surfaces with the reactive oxygen species (ROS) was done by Tengvall et al. [8], who actually evaluated if the metallic surface could enhance the inflammatory response promoting the

* Corresponding author at: Circuito Exterior sn, Ciudad Universitaria, Coyoacan, México D. F. 04510, México.

http://dx.doi.org/10.1016/j.msec.2016.04.035
0928-4931/

formation of oxidative species through a Fenton reaction. The conclusion from those works, where different metals (M) were compared, was that Ti (and most generally, the M^{4+} ions) does not contribute significantly to the formation of hydroxyl radicals even in a large pH window, which could partially explained the good biocompatibility of the M^{4+} metals. Moreover, they [8] propose that Ti surfaces immersed in H_2O_2 rich solutions, lead to the release of metal ions or TiO_2 species which are bound in a Ti–H_2O_2 complex inducing the formation of the TiOOH matrix that was not observed for any of the other metals. Since then, other works [7,9–13] have investigated the interaction of titanium surfaces with hydrogen peroxide, simulating the conditions when the metal is implanted in the human body and hydrogen peroxide is generated by an inflammatory reaction. Most of the analyses include the electrochemical evaluation of Ti surfaces immersed in simulated inflammatory conditions with H_2O_2 concentrations in the 10 to 330 mM. The reason behind these studies is that in vivo studies based on retrieved implants have shown that the thickness of the titanium oxide is much thicker than the passive stable oxide TiO_x film [14] that is spontaneously formed on metallic Ti surfaces, normally a few 5–10 nm thick [15]. And also thicker that the oxide layer formed during in vitro experiments where Ti was immersed on standard physiological solutions even in the presence of proteins. Pan et al. [16], found that the addition of H_2O_2 into the physiological solution where Ti pieces were immersed, leads to an increase in the dissolution/oxidation rate of titanium, evidenced by a decrease in the low frequency impedance of the Ti surface immediately after the immersion. However, after a few days, some regrowth or self-healing process was observed. By combining angle-resolved X-ray photoelectron spectroscopy, impedance spectroscopy and color interference analysis, they [16] concluded that H_2O_2 directed the formation of a surface double-layer. The formation of such a complex interface: thin-compact TiO_x (about 10 nm) followed by a thick (30 nm) porous (TiOOH) layer [7,8] is followed by the enhanced dissolution of metal ions due to the H_2O_2, which precipitates on the surface forming the porous outer layer [12]. The particular properties of the thick oxide layer grown during the vivo conditions could explain not only the larger biocompatibility of Ti in comparison to other metallic surfaces, but also the close contact between the bone and the implant obtained for Ti in comparison to other metals, with a certain degree of interlocking due to the porosity and roughness of the surface TiO_x layer. More recent studies have also investigated the Ti–H_2O_2 interaction, obtaining similar conclusions. Fonseca et al. [9] performed a complete electrochemical analysis, confirming the decrease in the corrosion resistance of the titanium in the presence of H_2O_2, and showing that there is an outer layer which is rougher and less blocking that the oxide formed in the absence of the oxidant. Bearing et al. [13] did a simultaneous electrochemical atomic force microscopy for Ti samples immersed in phosphate buffer solution containing 30 mM of H_2O_2. The conclusions were that the growth of the oxide domes was larger in the pure PBS than in PBS + H_2O_2, i.e. the oxidation resistance of the titanium was reduced in the presence of H_2O_2. Bearing et al. [13] actually compared cpTi with TiAlV, showing less reactivity of the alloy. However, Brooks et al. [12] observed a similar electrochemical response between cpTi and TiAlV, when immersed in solutions that simulate the inflammatory conditions (PBS + 150 mM H_2O_2 and pH = 5.0). Electrochemical impedance analysis indicated a decrease in the polarization resistance with an increase in the magnitude of the capacitance of the surface layer, which was associated to the formation of a thin and defective oxide layer. Moreover, they [12] also measured the amount of metallic ions released from the surfaces, finding that there was a significant increase in the dissolution of Ti ions into the solution in the presence of H_2O_2, phenomena that had been presumed in previous experiments but not directly measured. Such results are in agreement with the proposed model of Tengvall et al. [17], for the remodeling of the Ti surface through a dissolution–oxidation process. Hydrogen peroxide has also been proposed as a method to modify and improve the biological response of Ti surfaces based on H_2O_2 treatments. Karthega et al. [10] showed that the modification induced on Ti surfaces were dependent on the concentration of H_2O_2. In that case the immersion on H_2O_2 solution was done at 80 °C for 1 h and followed by an annealing at 400 °C and under this condition the oxide film grew with a specific structure that allowed the formation of a calcium phosphate layer on the surface.

All these previous studies demonstrate that titanium surfaces are highly sensitive to the interaction with H_2O_2 rich solutions. However, there are still some details of the interaction that have not been explored, as for example the effect of the peroxide on other surface properties. Surface properties include many aspects such as wettability, surface energy, roughness, composition, crystallinity, etc. [18] and many of them have been shown to be determinant factors for the cellular adhesion, proliferation and differentiation [5,19–22].

The aim of the present paper is to evaluate the variations induced in the physico-chemical properties of the titanium surface as a consequence of the immersion for 7 days in H_2O_2 rich solutions and compare such variations with those occurring in a less biocompatible metal, such as the medical grade stainless steel (AISI 316L). The approach is different than in previous studies, since the samples will be exposed to the H_2O_2 rich solutions, washed and then, the surface physico-chemical properties will be evaluated, including the difference in the electrochemical response.

It is worth to mention that the use of H_2O_2 solutions to simulate the inflammatory process occurring in vivo is an over simplification of the real process, which involves not only one chemical reactive specie but also the inflammatory cell response. The release of reactive oxygen species (ROS) by inflammatory cells in response to biomaterials in vitro have been measured by different authors [23–27] and in-vivo real-time generation of ROS were measured over the course of 28 days [28]. Moreover, the authors [28] found that high levels of ROS were histologically correlated with the presence of phagocytic cells and fibrosis at early and later times, respectively, suggesting that ROS may be involved in both the acute and chronic phase of the foreign body response. Despite all these works, not quantitative data about the concentration of ROS or H_2O_2 are usually reported; the results are presented as relative data, indicating more or less ROS. Therefore, for the present work, we chose a concentration within the range reported by Tengvall et al. [17].

2. Experimental details

2.1. Sample and films preparation

Disks of both titanium grade 2 (cpTi, 14 ϕ mm × 1.2 mm) and 316L stainless steel (SS, 13.5 ϕ mm × 1.2 mm) were polished using 80, 120, 220, 360, 600, 1000, 1500 and 2000-grit silicon carbide paper, and finished in automatic polishing machine (UNIPOL-810 MTI) using 1 and 0.3 μm alumina suspensions. Then, the disks were washed and sonicated consecutively during 10 min in acetone, isopropanol and deionized water, finally, they were dried with nitrogen gas.

2.2. Hydrogen peroxide treatment

The H_2O_2 treatment consists of the immersion of the samples during 7 days in a Hartman® solution containing 50 mM of H_2O_2. The samples were immersed in 15.0 mL of this solution and kept in dark at 37 °C during 7 days; only the top surface was exposed by masking the counter face with silicon coating. The solution was refreshed every 24 h to avoid the loss of the H_2O_2 species; according to the measurements of Pan et al. [7] using a VACUette ampoule test, the H_2O_2 concentration decreased about 40% of the initial value in 24 h. Finally the samples were washed using deionized water and dried with nitrogen. Samples before the treatment are named pristine (P) and after the treatment, they have been name as treated-samples (T), then the labels used along the paper are cpTi-P, cpTi-T, SS-P and SS-T. For reference, immersion experiments for 7 days in pure Hartman solution were also performed, but no significant changes in the surfaces properties or the electrochemical response

were observed. As mentioned in the introduction, the 50 mM hydrogen peroxide concentration was chosen based on previous reports [17], but we did also some screening experiments using 20 mM and 100 mM. The first concentration did not induced significant changes on the surface, while the 100 mM was too aggressive, leading to extended corrosion of the SS sample.

2.3. Physico-chemical surface characterization

The chemical composition of the pristine and treated samples was measured using the K-Alpha X-ray photoelectron spectrometer (XPS) by Thermo Fischer Scientific. An argon beam was used to clean the surfaces before the XPS analysis. The XPS was operated at 8×10^{-7} Pa using Al Kα radiation $h\nu = 1486.6$ eV with a spatial resolution of 500 μm and 200 and 25 eV pass energy to acquire the survey and high resolution spectra, respectively.

The surface topography and roughness of P and T samples were measured by atomic force microscopy (AFM) using a Jeol JSPM-5200. The sample scanning was performed using the tapping mode at ambient conditions. The cantilevers used were a V-shaped silicon model NSC15 with a vertex angle of 20° and a radius of curvature of 10 nm with a shape of a square pyramidal. The areas of scanning were 5 × 5 μm. The roughness was also measured using a DEKTAK II profilometer; seven different scans of 250 μm length were done on three samples of the same type.

The contact angle was determined using a Ramé-Hart Inc. Goniometer in static sessile drop mode; drops of 5 μL were used for each probe liquid. Three liquids were employed: water, formamide and diiodomethane. Previous to the measurements, all samples were exposed to the same cleaning process consisting of sonication in isopropanol, drying using nitrogen and heating by 15 min at 80 °C.

The calculation of the surface energy was performed using the Van Oss–Chaudhury–Good (VCG) [29–32] method:

$$(1 + \cos\theta)\gamma_L = 2\left(\sqrt{\gamma_S^{LW}\gamma_L^{LW}} + \sqrt{\gamma_S^{+}\gamma_L^{-}} + \sqrt{\gamma_S^{-}\gamma_L^{+}}\right)$$

where θ is the contact angle, γ_L the total surface tension of the probe liquid, γ_S^{LW} *and* γ_L^{LW} are the non-polar or dispersive interaction (Lifshitz van der Waals) of solid and probe liquid, respectively. The polar interaction, γ_S^{AB} was decomposed into its Lewis-acid and Lewis-base components; $\gamma_L^{+}\gamma_L^{-}$ and $\gamma_S^{+}\gamma_S^{-}$, respectively.

The point of zero charge (pzc) was also determined before and after the treatment. For this, we use potentiometric titration, using 0.01 M KCl as a background electrolyte, whose initial pH value was adjusted with solution 0.01 M HCl to obtain a pH value of 2. The purpose of the background electrolyte was to stabilize the ionic strength in the solution, and it was selected considering that the cations and anions of the background electrolyte do not compete with the adsorption process and do not react with the catalyst surface generating complexes in the solution. The titration was carried out by adding 2 mL of 0.01 M NaOH and measuring the change in the pH (from 2 to 12), using a potentiometer (Jeanway model 3540) and bubbling nitrogen. Finally, the change of pH as a function of added volume of NaOH represents a curve in which its inflection point is the pzc [33,34].

2.4. Electrochemical measurements

Electrochemical experiments were performed in a classical three-electrode cell of 150 mL at room temperature using a PCI400 Gamry potentiostat. The reference electrode was a calomel electrode (SCE, Hg:HgCl), the counter electrode was a platinum wire of 5 mm of diameter and 10 cm in length, and the samples functioned as the working electrodes. The area exposed for each sample was of 0.196 cm^2. The electrolyte was the Hartmann's solution that simulates physiological fluid. Hartman solution was chosen since it is a standard medical solution isotonic with blood; it simulates the mineral concentration of the physiological fluids. Basically, it contains sodium (131 mEq), chloride (111 mEq), potassium (5 mEq) and calcium (4 mEq) ions plus lactic acid. Lactic acid (2-hydroxypropanoic acid) is a chemical compound involved in a variety of biochemical processes. The concentration of lactate in the Hartman solution is 29 mmol/L similar to the concentration of lactated Ringer's solution that is another solution commonly used to simulate corrosion processes in physiological fluids.

Each sample was immersed in the electrolytic cell and the open circuit voltage (OCP) was monitored for at least 1800 s, where it usually has reached the equilibrium. Then, the electrochemical impedance spectroscopy (EIS) experiment was initiated. Impedance data were collected versus SCE, in the frequency range from 0.01 Hz to 100 kHz at AC electrical signal of 10 mV for all the samples. At the end, the impedance spectra were recollected a second time to make sure that no variation was induced to the surface during the EIS acquisition. If this condition was fulfilled, then the potentiodynamic polarization (PP) measurements were performed. The voltage scan was done from −1 V to 1 V using a steep rate of 0.5 mV/s.

Data analysis was performed using the software Gamry Echem Analyst. The corrosion potential, E_{corr}, and corrosion current density, I_{corr}, were calculated by the cathodic Tafel slope. Meanwhile the EIS spectra were fitted using appropriate equivalent circuits and the Levenberg–Marquardt algorithm. For all the EIS data, a Kramers–Kroning analysis was performed to confirm the validity of the measurements before proceeding with the equivalent circuit analysis [35].

2.5. Statistical analysis

All measurements were done by triplicate (3 different samples); for AFM and Electrochemical tests, only one measurement for sample was done. For profilometry, seven scans were done on each sample (number of total data = 21). For contact angle, two drops were measured in each sample and the left and right angles were calculated, leading to 12 angles for each liquid. The final results were analyzed using the IBM-SPSS software. For the results that showed a normal distribution (AFM, profilometry for cpTi, wettability and electrochemical tests), the paired *t*-test was used, so the mean values and standard errors are reported. When, the results did not show a normal distribution (profilometry for SS and surfaces energies), the Wilcox-signed rank test was used and so the median values were used to compare between groups; standard errors are also reported.

3. Results

3.1. Chemical composition

Fig. 1a–d shows the XPS results from the two samples before (a–b) and after (c–d) the immersion in the H_2O_2 enriched Hartman solution. It can be seen that the surface composition of both metallic surfaces were strongly modified. The untreated cpTi-P (1a) showed the presence of both metallic Ti (Ti^0 $2p_{1/2}$ and Ti^0 $2p_{3/2}$peaks, 75%) and a sub-stoichiometric TiO_x oxide (Ti^{2+} $2p_{1/2}$ and Ti^{2+} $2p_{3/2}$ peaks, 25%) [36]. The detection of metallic Ti could be associated to the small thickness of the native oxide layer of the Ti, which is usually reported as 5–10 nm, therefore some photoelectrons emitted from the under-layer metallic Ti can reach the detector or, to a non-uniform native oxide layer. However, the results also indicated that the native oxide surface layer does not have the stoichiometric TiO_2 composition. After the 7 days of immersion, the amount of metallic Ti was strongly reduced (11%) and the dominant peaks correspond to $Ti^{4+}2p_{1/2}$ and $Ti^{4+}2p_{3/2}$ (63%) suggesting that the native oxide has become stoichiometric (TiO_2) and probably thicker, so the metallic Ti signal is reduced. For the SS, the analysis was focused on the chromium signal since the surface layer of SS is predominantly a chromium oxide. Similarly to the cpTi, we found signals from both metallic Cr ($Cr^0 2p_{1/2}$ and $Cr^0 2p_{3/2}$, 58%) and Cr_2O_3 ($Cr^{3+}2p_{1/2}$ and Cr^{3+} $2p_{3/2}$, 42%) in the polished SS (Fig. 1b). However, after the immersion, only the Cr_2O_3 signal was detected.

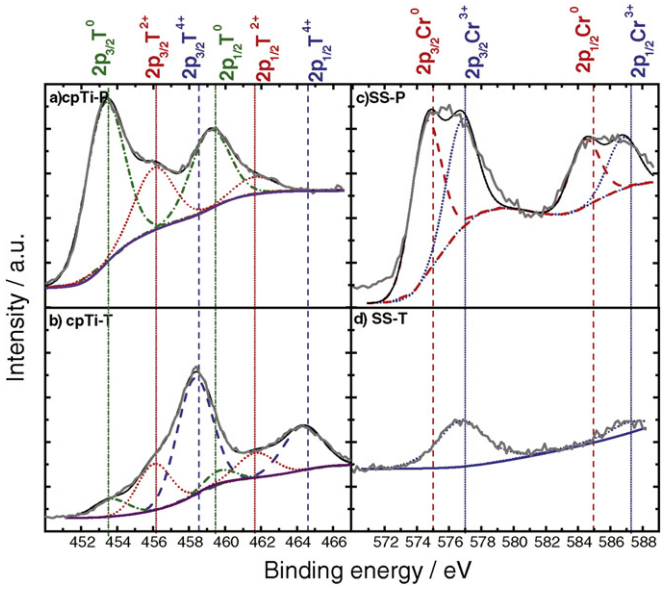

Fig. 1. Elemental analysis before and after the treatment performed by X-ray photoelectron spectroscopy. The 2p Ti peaks in titanium for (a) cpTi-P, (b) cpTi-T, and the Cr 2p peaks for (c) SS-P and (d) SS-T.

In the two metallic samples, oxidation of the surface was promoted and/or the oxide layer was thicker after the immersion.

3.2. Topography and roughness

Fig. 2a–d shows the atomic force microscopy images at 5 × 5 μm resolution of the four samples before (a–b) and after (c–d) immersion. Some scratches related to the polishing process can be observed. After the treatment, both surfaces presented more regular spikes than before but in general not very strong variations on the surface topography were induced by the H_2O_2, probably due to the relative low concentration used (50 mM). Nevertheless, the quantitative analysis of the surface topography indicated that the roughness parameters (average roughness, R_a; root mean square roughness, R_q and the average 5 largest peak-to-valley values, R_{zjis}) nearly doubled for the cpTi, while for the SS the variations were lower, data shown in Fig. 2. It has been extensively demonstrated by Giljean et al. [37] and others [38] that a priori it is not obvious which is the roughness parameter that is important for an specific cell–surface interaction, such as the attachment, adhesion, proliferation or differentiation. On the other hand, roughness values are also dependent on the length scale, and then scan dimensions in accordance to the size of the biological entities should be used. According to the analysis of Bigerelle et al. [39], 2D profilometry analyses are more adequate to correlate surface parameters with surface-cell interactions than AFM. Then, roughness amplitude parameters were measured at a length scale of 250 μm using a contact profilometry. Since the length scale is much larger using the profilometry than for AFM (250 μm vs 5 μm), the estimated roughness data are different among both techniques. Fig. 3 shows the R_a, R_q and the R_{zjis} for the cpTi and SS samples before and after the treatment. Even though both samples were mirror-polished, the roughness was one order of magnitude higher on the cpTi than for the SS, most probably due to the difference on their mechanical and synthesis parameters. From this figure and the statistical analysis ($p < 0.05$), we are certain that there was an increase in the surface amplitude parameters for both samples after the treatment. The increment in surface roughness was about 65–100% (different for each parameter and material) of the initial value for both samples, in agreement with variations observed using the AFM at lower length scales. The statistical analysis indicated that all the changes were statistically significant ($p < 0.05$).

3.3. Water wettability and surface energy

The mean water contact angles (WCA) or wettability are shown in Fig. 4. The results indicated that the untreated surfaces have WCA between 61

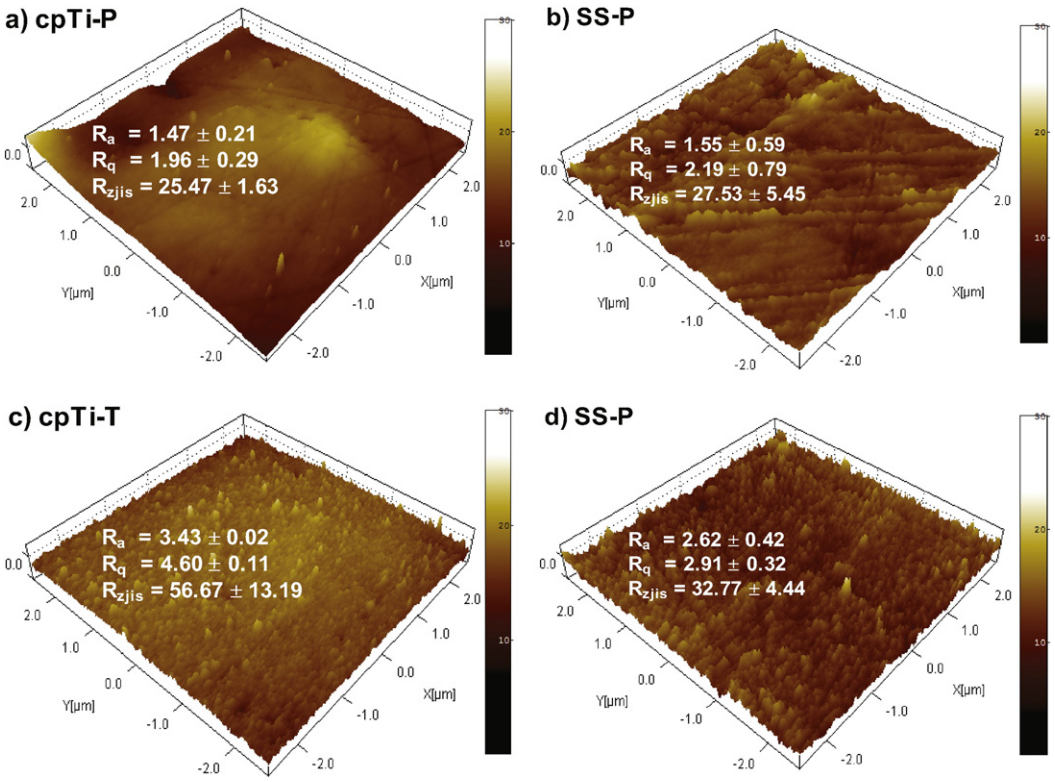

Fig. 2. Atomic force microscopy (mean values ± standard error) measured at 5 μm × 5 μm amplification before (a) cpTi-P and (b) SS-P and; after the treatment (c) cpTi-T and (d) SS-T. All the roughness values are given in nm.

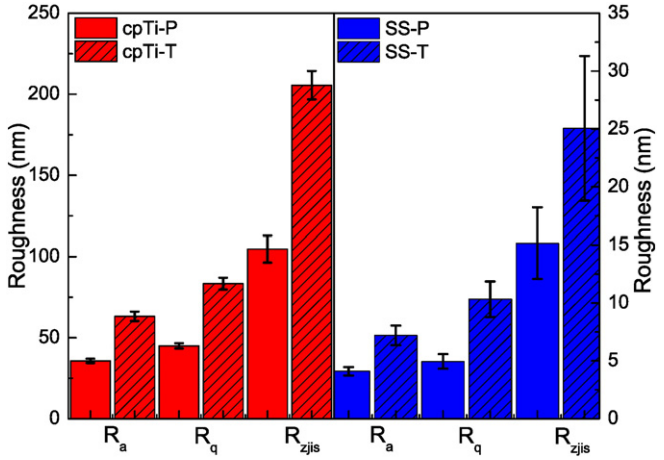

Fig. 3. Roughness values obtained by profilometry (250 μm scan length) for both surfaces before and after the treatment: R_a is the average roughness, R_q is the root mean square value and R_{zjis} is the average 5 largest peak-to-valley values. For cpTi; mean values ± standard error, while for SS median values ± standard error are shown. Roughness parameters increased after the treatment for both samples.

and 65° which according to Berg et al. [40] and Vogler E. A. [41] are close to the limit between hydrophobic and hydrophilic surfaces. After the immersion, the WCAs were significantly ($p < 0.05$) reduced for both surfaces, but the effect was stronger for cpTi (from 61.5° ± 1.5° to 36.2° ± 2.5°) and much lower in SS (65.2° ± 0.7° to 50.5° ± 0.5°); both changed to a more hydrophilic character. The water contact angles measured for the cpTi are in good agreement to those reported by other authors; Ponsonnet et al. [42] reported 53.9° ± 5.1°, Mekayarajjananonth and Winkler [43] reported 58.5° and Rosales-Leal et al. [44] obtained about 62° ± 4°, even though it is well known that WCAs are dependent on the cleaning procedure, so large difference can be reported for the same material [45,46]. The decrement in the WCA is on agreement with the slight increment observed in the solid/liquid interfacial tension (the work of adhesion), γ_{sl} calculated using both the Young–Dupré and VCG method, data reported in Table 1. The observed change of the cpTi through more hydrophilic character is in principle a good factor to promote cell interaction and the in vivo rate of osseointegration [47–50]. However, it is important to consider that the surface wettability is usually working synergistically with other surface properties, such as topography, surface energy and charge.

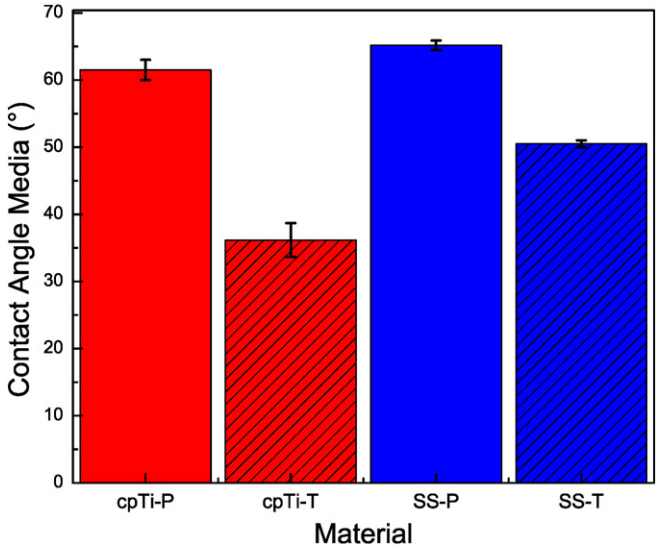

Fig. 4. Water contact angle (mean values ± standard error) or wettability of cpTi and SS before and after the treatment. Both samples are more hydrophilic after the treatment.

Table 1
Solid–liquid interfacial energy calculated by two different methods using the water contact angle data.

Material	$\gamma_{S\text{-}Water}$[a] mJ/m^2	$\gamma_{S\text{-}Water}$[b] mJ/m^2
cpTi-P	107.90 ± 0.02	107.5 ± 1.5
cpTi-T	131.40 ± 0.04	131.6 ± 2.5
SS-P	103.50 ± 0.01	103.4 ± 0.7
SS-T	118.90 ± 0.03	119.1 ± 0.5

[a] Van Oss–Chaudhury.
[b] Young–Dupré.

In order to obtain information about the surface energy of the solid using the Liftshitz–van der Waals/acid–base approach, the VCG method was used using the contact angles measured for three liquids (water, diiodomethane and formamide). Fig. 5a–d shows the histograms for the total surface energy (5a), the dispersive or non-polar component (5b), the polar component (5c) and the acidic (5d) and basic (5e) components. The total surface energy and the dispersive component before the treatment were similar for both metallic surfaces; in agreement with reported values [42,51]. After the treatment, the total and dispersive energies showed the same trend; they increased slightly for cpTi and decreased for the SS. The increase in surface energy indicates that the surface reactivity has also increased and therefore chemical or physical adsorption will occur more easily after the treatment. It has been extensively shown that hydrophilicity affects positively the amount of adsorbed proteins and their conformation and orientation [52–54]. Protein adsorption is considered the initial surface-medium interaction and it creates a preconditioned surface that later defines the cell response [41,55].

Larger and significant changes were detected for the polar component (5c). The polar component increased for SS (5.3 to 7.7 mJ/m^2) and decreased for the cpTi (6.5 to 4.8 mJ/m^2). The variations in the electron-acceptor (Lewis-acidic, γ^+) and the electron-donor (Lewis-base, γ^-) components are shown in Fig. 5d and Fig. 5e, respectively. The acidic constituent (γ^+) decreased after the treatment; the variation was stronger for the cpTi than for the SS. In accordance, the basic constituent (γ^-) of the cpTi was nearly threefold after the treatment and the value for SS was doubled; i.e. the electron-donor character was increased for both samples. The electron-donor/electron-acceptor interactions have been correlated to various interfacial phenomena such as phagocytosis, protein adsorption [32,56] and microbial adhesion [57]. However, less is known about their effect on cell membranes.

3.4. Surface charge (point of zero charge)

The surface point of zero charge was measured before and after the H_2O_2 treatment and the results are reported in Fig. 6. The pzc describes the solution pH at which the electrical density on the surface is zero and accordingly, it determines the surface charge of the material at physiological pH values [34]. The data indicated that the pzc increased after the treatment for both samples in agreement with the increase in the basic character of the polar component of the surface energy. The largest the basic character means that the surface has a more positive character, then when the surface is submerged in aqueous solutions, to compensate the positive charge on the surface, it requires a larger adsorption of negative or hydroxyl ions (OH^-), i.e. the pH to get a zero surface charge is larger. Moreover, the result is in agreement with previous reports, where the pzc of clean, hydrated Ti surface is close to 6.7. The significance of these results, is that after the treatment, the cpTi will be less charged at the physiological conditions (pH = 7) than before. Meanwhile the SS will be more charged than in the pristine condition. The pzc value of SS increased slightly from 7.3 to 7.6; at physiological conditions (pH = 7) it will be more positively charged, while the cpTi will be less negatively charged. This different behavior might have important consequences for the cell–surface and cell–protein interactions, since

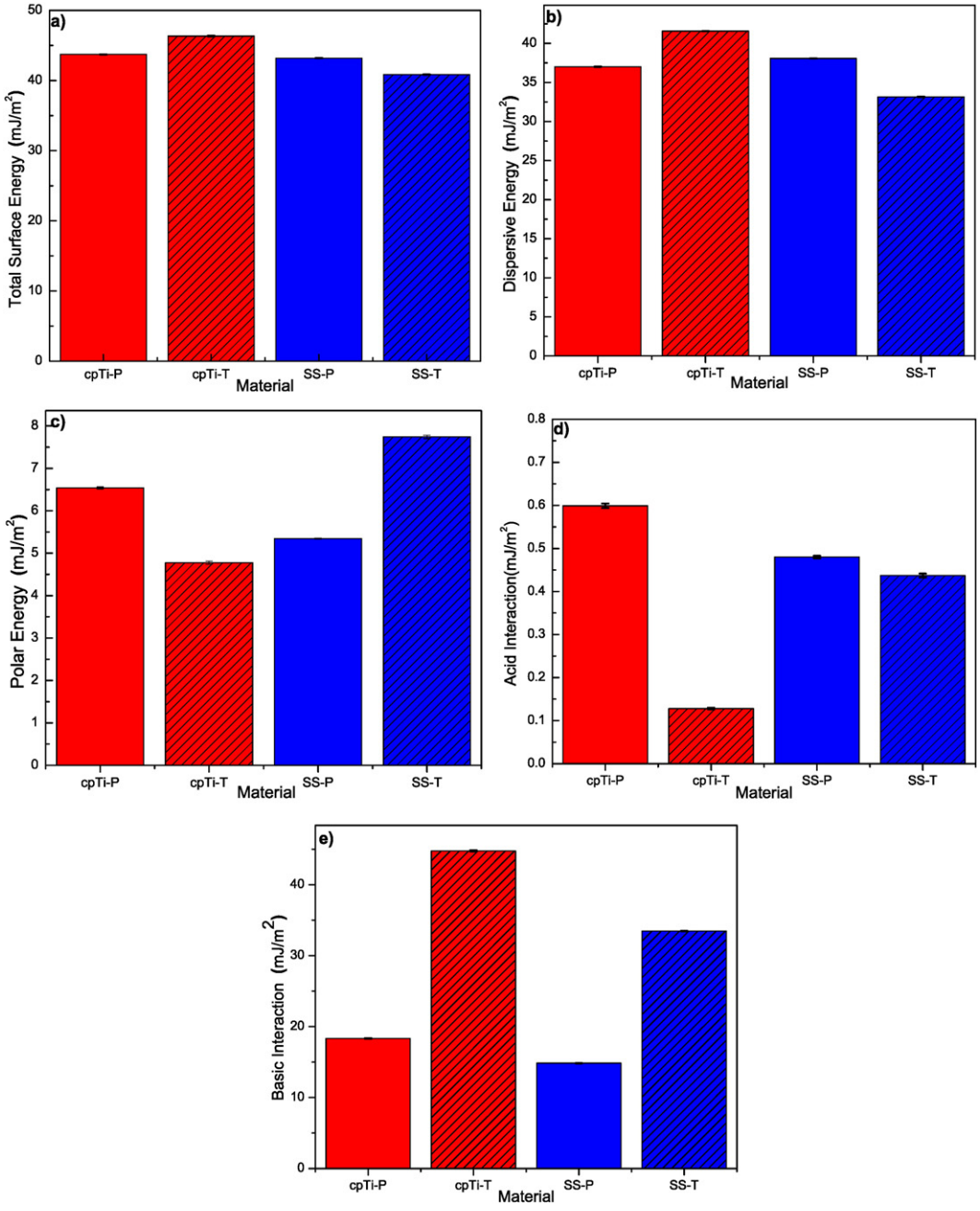

Fig. 5. Surface energy (media values ± standard error) calculated using the Van Oss approach: (a) total surface energy, (b) dispersive component, (c) polar component, (d) acid component and (e) basic component.

strong electrostatic interactions between the implant surface and the biomolecules are not favorable to improve the biocompatibility. For example, the cell membrane is negatively charged due to its high composition of negatively charged lipids, thus strong electrostatic interaction might lead to rupture of the cell membrane and severe toxicity.

3.5. Electrochemical evaluation

3.5.1. Open circuit potential

The open circuit potential (OCP) was measured as a function of time for both samples, up to 1800 s, where a stable value was obtained (Supporting Information Fig. S1). The OCP changed from negative to positive after the treatment; for the cp-Ti, it increased from approximately −60 mV to +50 mV and for the SS from −24 mV to +62 mV. Both surface showed a more passive behavior, probably due to the formation of the thicker or stoichiometric oxide layer after the interaction with the H_2O_2 rich solution.

3.5.2. Impedance spectroscopy

Immediately after the OCP stabilization, the impedance spectra were acquired. Representative Bode (averaged magnitude and phase) and Nyquist plots from the EIS tests for the two samples before and after the H_2O_2 treatment are shown in Fig. 7a–d, respectively. From the Bode plots, it can be seen that the impedance values at low frequency drastically decreased after the treatment for the cpTi, while it was not changed for the SS. Similarly, not changes were observed for the phase angle of the pristine and treated SS samples; ~70° in the middle range frequency. The phase angle for the pristine cpTi was about 80° in a wide window of frequencies (highly capacitive behavior of the native oxide), but after

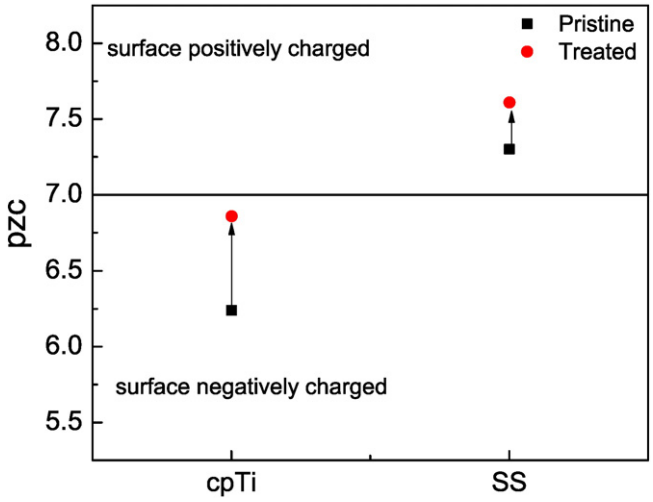

Fig. 6. Variation of the point of zero charge due to the immersion in H_2O_2 rich solutions. The relative charge of the surfaces in relation to the neutral pH is indicated.

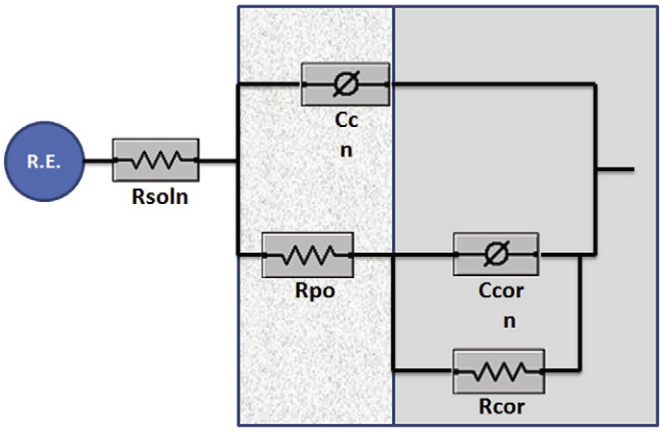

Fig. 8. Equivalent circuit diagram used to model the impedance spectra of both surfaces before and after the H_2O_2 treatment.

the treatment decreased to ~70° and the frequency window was reduced, suggesting the formation of the outer porous layer.

The Nyquist plots clearly show that there is almost no variation of the electrochemical response for the SS; the diameter of the semicircular capacitive loop remained unchanged within the experimental error. Meanwhile, for the treated cp-Ti the diameter was significantly reduced; an amplification of the high-frequency region is shown in the inset of Fig. 7c.

Quantitative data was obtained by fitting the impedance spectra using the circuit model shown in Fig. 8 which contains the solution resistance in series with two parallel (R,Q) circuits, where the Rs are resistance elements, and the Qs constant phase elements (CPE). The impedance of the CPEs are $Z = 1 / Q(jw)^n$ where n is typically between 0.5 and 1. Values of n equal to 1, means that the CPE is an ideal capacitor, while n lower than one account for non-uniform current densities due to surface roughness or inhomogeneity, such as variation of the resistivity along the thickness of the surface film [58–60]. This circuit has been shown to work well for passivated metals such as SS and Titanium [61]. Other authors, however, used single Randles circuit [12,62,63] to model a compact native oxide, but in our case, it did not work for any of the two surfaces.

The first RQ (R_{po},Q_c) in Fig. 8 simulates the resistance and capacitance of the outer interface; the passive oxide in the metallic surface. The second RQ circuit simulates the electrolyte–substrate interface (R_{cor},Q_{cor}) that corresponds to the faradic processes leading to the dissolution of the metallic substrate; R_{cor} is the corrosion resistance of the metallic substrate and (Q_{cor}, n) is the CPE associated to that interface. Examination of the fitted data (Data in Table S1 of the supporting information) is shown in Fig. 9 that shows that both the corrosion resistance (R_{cor}) and the pore resistance (R_{po}) significantly ($p < 0.05$) decreased for cpTi, while both resistances were not significantly different for the SS. The R_{po} describes the easiness for the transport of oxygen and metal ions through the outer layer. Therefore, the lower R_{cor} for the cpTi is

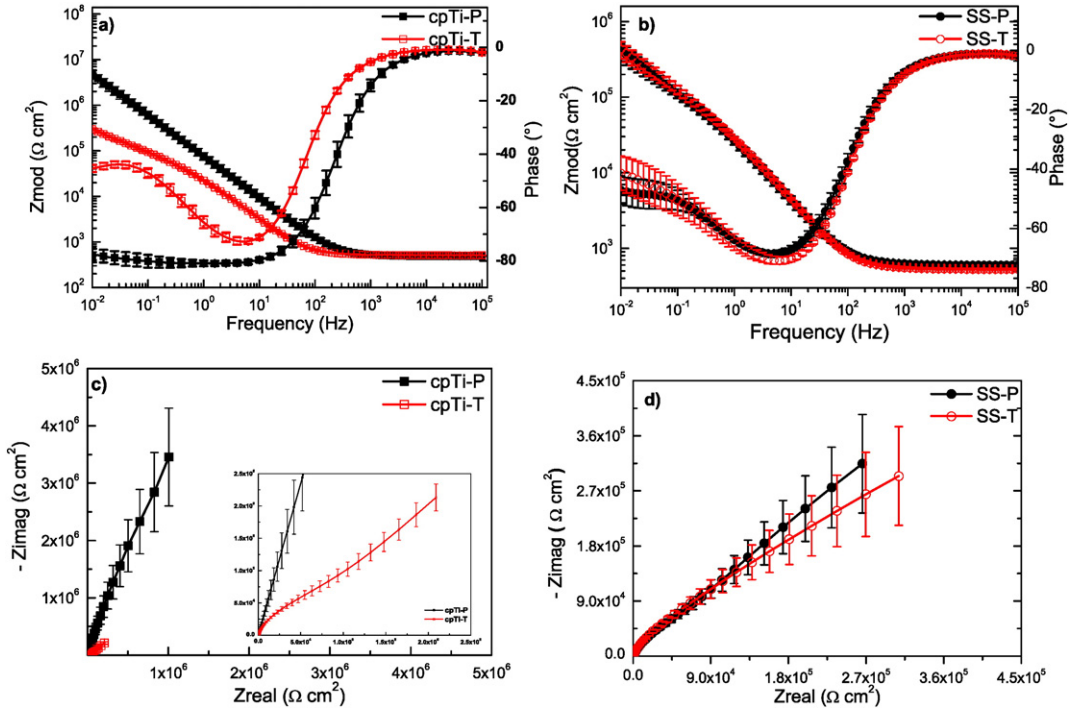

Fig. 7. Data obtained from the impedance spectroscopy (averaged curves ± standard error) before and after the treatment; Bode plots for (a) cpTi and (b) SS; Nyquist plots for (c) cpTi and (d) SS.

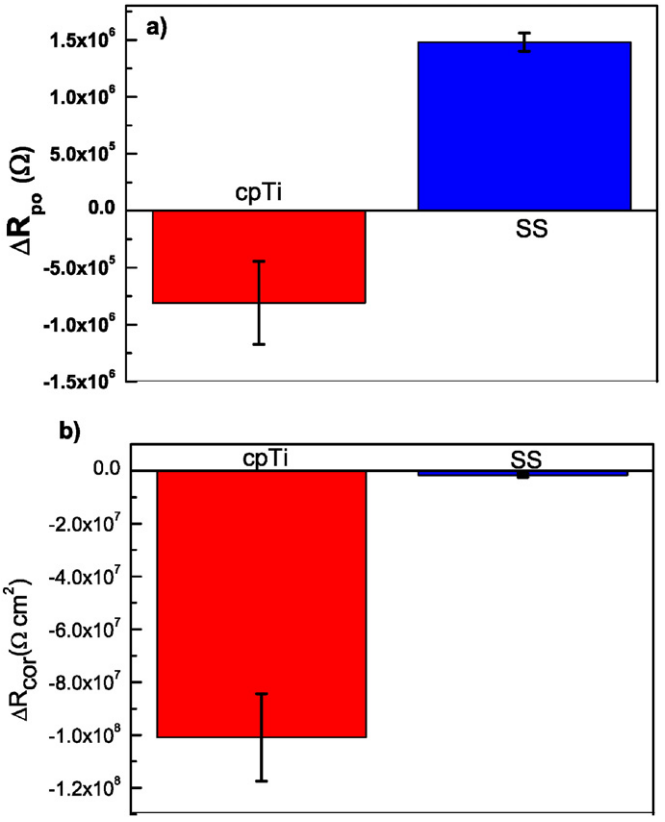

Fig. 9. Difference in the polarization resistance (ΔR_{po}) and the corrosion resistance (ΔR_{cor}) as a consequence of the treatment.

an indicative of a higher dissolution, while the lower R_{po} means that the species are easily transported though the outer layer, which can be explained in terms of a porous TiO_x layer. For the cpTi, both capacitances are also significantly ($p < 0.05$) increased, i.e. lower corrosion resistance after the treatment. The trend for the SS is a slight reduction in both capacitances, but the difference is no statistically significant. The deviation of the exponent parameters of the CPEs from 1 have been proposed as indicative of either larger surface roughness [64], the presence of a porous corrosion product layer or heterogeneities on the surface [59]. The results indicated that the exponents were always closer to 1 for the cp-Ti in comparison to the SS, but as shown in Fig. 3, the roughness was larger for the cpTi, so maybe the lower values obtained for the SS ($n = 0.58$ and $m = 0.86$) are indicative of a larger surface heterogeneity. After the treatment, the exponent decreased slightly but the statistical analysis showed that the variation between pristine and treated samples were not significant ($p < 0.05$).

3.5.3. Potentiodynamic polarization

Finally, after the EIS measurements that last about 2 h per sample, the potentiodynamic polarization (PP) curves were obtained. The PP plots are shown in Fig. 10 from −1.0 to 1.0 V which allows us to observe the differences in the passivation behavior of the samples. The passivation window is larger for the cp-Ti in comparison to the SS; a clear critical current density $I_{crit} = 2.5 \times 10^{-6}$ A/cm^2 is observed for the SS around 0.8 V, while a slow dissolution is observed for the cpTi and such behavior is similar before and after the treatment. From the PP curves, the I_{corr}, E_{corr} and cathodic tafel slopes were obtained and reported in Table 2. The most significant variation was obtained for the corrosion current density that increased for the cpTi while it remained nearly unchanged for the SS. The corrosion current density is directly proportional to the corrosion rate, so this result indicates that after the immersion the titanium surface is more prompt to suffer corrosion. The

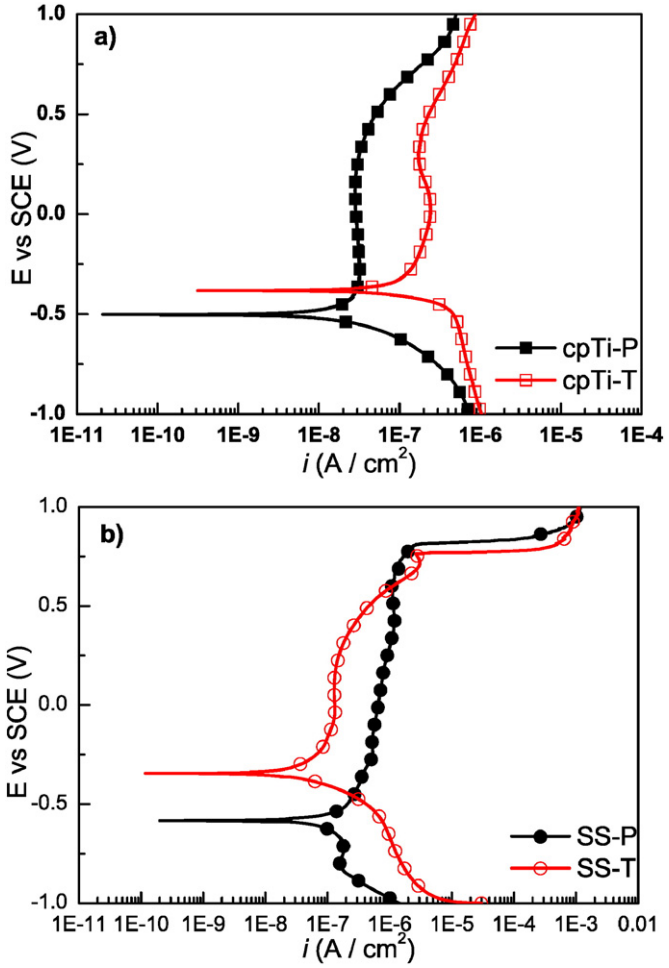

Fig. 10. Potentiodynamic polarization curves for (a) cpTi and (b) SS before and after the treatment.

cathodic Tafel slopes were similar after the treatment for both materials, but the initial value was smaller for the SS than for cpTi.

4. Discussion

The objective of the study was to compare how immersion into H_2O_2 rich solutions (simulated inflammatory conditions) alters both the surface properties and the electrochemical response of pure titanium and medical grade stainless steel. To achieve this, we measured a wide range of physico-chemical surface properties and performed electrochemical tests before and after the immersion. The aim of the comparison was to gain understanding about why Ti surfaces have a better biological outcome in comparison to stainless steel, through recognizing their different in vitro response to exposure to the immersion into inflammatory physiological conditions. Since the 1960s Ti and its alloys have been extensively used in dentistry, orthopedic and maxillofacial

Table 2
Results (mean values ± standard error) for the cathodic slope, corrosion potential and corrosion current density determined from the potentiodynamic polarization of the cpTi and SS before and after the treatment measured using the Hartman solution as the electrolyte.

Material	β_C V/decade	E_{cor} mV	I_{cor} nA/cm^2
cpTi-P	0.09 ± 0.01	−451.7 ± 26.4	7.1 ± 0.3
cpTi-T	0.10 ± 0.01	−374.5 ± 8.5	47.2 ± 8.3
SS-P	0.09 ± 0.01	−544.6 ± 98.5	29.6 ± 5.5
SS-T	0.08 ± 0.01	−447.7 ± 88.6	31.1 ± 18.0

reconstructive surgery; one of the reasons is the high corrosion resistance provided by the TiO_x native oxide layer that forms spontaneously on the surface when exposed to air and solutions [62]. Moreover, studies from extracted implants have shown the growth of a thicker TiO_2 layer in the in vivo conditions [14,65]; the oxidation of the Ti surface is larger than the observed values for in vitro experiments even when complex biological electrolytes were used [61,66]. A plausible explanation for the increase oxidation rate was given as a consequence of the chemical environment to which the implant is exposed after the surgery, where usually an inflammatory response is triggered. When biomaterials are implanted a series of events occurs as described in many review papers [67–69]. The surgical wounding is enough to activate the immune system, which comprises cells and mechanisms to defend the host from infection by other organisms or damage to tissue integrity [70–72]. Inflammation is one of the first responses of the immune system, it serves to both avoid infections and start wound healing. Molecules produced during inflammation attract the cell response attracting phagocytes, especially neutrophils and macrophages.

Neutrophils characterize the acute inflammatory response, which for biomaterials is usually resolved in one week [67]. During this stage, reactive oxygen intermediates (ROIs) are produced to kill microbes in a series of reactions initiated by enzyme complexes, such as NADPH (nicotinamide adenine dinucleotide phosphate) which can create superoxide ($O_2^{\bullet -}$) from molecular oxygen [70]. The superoxide functions as a substrate for the generation of hydrogen peroxide, which can react with the superoxide to form also hydroxyl radicals following the next reactions [70]

$$2O_2 + NADPH \rightarrow 2O_2^{\bullet -} + NADPH + H^+$$

$$2H^+ + 2O_2^{\bullet -} \rightarrow H_2O_2 + O_2$$

$$O_2^{\bullet -} + H_2O_2 \rightarrow OH^{\bullet} + OH^- + O_2.$$

Since the effect of the biomaterials cannot be controlled by this method, i.e. as a normal infection by microorganisms, the chronic inflammation process proceed. Chronic inflammation is identified by the presence of macrophages at the implant site. Macrophages experience what is known as “frustrated phagocytosis” since they cannot engulf the intruder [73]. They fuse to form foreign body giant cells covering the surface of the implant and creating a local micro-environment. Within this area, a myriad of degradation mediators are released, so again the surface of the biomaterial is exposed to low pH, ROIs, degradative enzymes and acids [67]. The final outcome is dictated by the size and chemistry of the biomaterial and its response to the degradation mediators. Material sizes smaller than 10 μm in diameter (size of a single macrophage) or biodegradable materials may be phagocytized by macrophages, resolving the inflammation process [67,73]. For bulk or no degradable materials, such as metallic implants, macrophages will fuse into foreign body giant cells and remain on the surface of the implanted material for the lifetime of the implant [67,73]. This is not necessary a negative outcome, since the ideal consequence of inflammation is wound healing and therefore macrophages also play an important role in angiogenesis [74]; growth of new blood vessels, which is critical for the integration of the implant to the surrounding tissue. However, the chemical changes induced on the surface of the biomaterial by the long-term oxidation process induced by the foreign body reaction described above should not be detrimental of the biomaterial's properties and stability.

In the results from this work, we see no direct evidence (not separate time constants are observed in the impedance spectra) of the formation of a double compact-porous oxidized titanium layer, as seen in the previous studies by Pan et al. [7,16] and Tengvall al. [8,17] The impedance spectra obtained after the H_2O_2 treatment did not require the addition of a third (R,Q) circuit to take into account the presence of the porous layer. This could be a consequence of the washing and drying process to which the samples were exposed after the 7-days of immersion or simply that the concentration and time was not large enough to induce stronger changes on the surface. However, our results indicated a single titanium oxide surface, thicker and more porous and defective than the initial native oxide; i.e., the corrosion resistance of the cpTi was reduced as a consequence of the interaction with the H_2O_2 rich solution in agreement with Pan et al. [7] and Tengvall et al. [17]. The increase in the thickness of the TiO_2 layer was inferred from both the XPS data and the decrease in the capacitance of the (R_{po},Q_c) circuit. XPS showed that after the treatment, the Ti (IV) was the unique oxidation state detected for Ti. On the other hand, it is well-known that the capacitance is inversely proportional to the thickness of the layer (*capacitance* $= \frac{\varepsilon\varepsilon_o A}{t}$; ε is the film dielectric constant, ε_o is the vacuum permittivity, A is the area and t is the thickness) and the Q_c value is proportional to the equivalent capacitance, so the decrease in the Q value suggested that the surface outer layer was thicker after the treatment. Since the exponent values of the CPEs were different to 1, suggesting that the formed film is not homogeneous in properties, it is not accurate to estimate the capacitance [59] and in consequence we could not estimate the thickness of the modified TiO_2 layer.

Concerning to the stainless steel surface, the results clearly indicated that in comparison to the cpTi, the surface of the SS was less modified by the interaction with H_2O_2; surface roughness and electrochemical response were very similar. Meanwhile, the surface composition (XPS) showed that a complete oxidation of the SS surface was obtained after the immersion in the H_2O_2 rich solution and some variations in the surface energy components were also observed. The apparent inertness of the SS sample, which might seem to be a good indicator of the stability of the surface when exposed to the physiological inflammatory conditions, might be indeed a detrimental factor for its biocompatibility [75]. The cpTi surface suffered from a dissolution/oxidation process that allows its integration with the surrounding media and as shown by other authors [7,9,13,17], such process leads to higher corrosion resistance in the long time. However, the SS does not adapt with the surrounding media, it retained basically the same properties. Moreover, the few changes are not favorable; the pzc value moved a little bit away from the neutral pH, meaning that at pH = 7, the SS surface will have a slightly higher positive charge on the surface after the treatment, inversely to cpTi, where the pzc moves closer to the neutral pH after the treatment. The higher charge on the surface of SS will increase the electrostatic interaction with macromolecules (proteins) increasing the possibility of conformational damage during adsorption, which will eventually affect the cellular adhesion [76].

A significant different answer between SS and cpTi was observed for the surface energies; after the treatment, the dispersive component increased for cpTi, while it decreased for SS and inversely, the polar component decreased for cpTi and increased for SS. The effect of the dispersive component on the cell–surface interactions has not been deeply studied, however, Ponsonnet et al. [42] and references therein, have shown that fibroblast adhesion and proliferation is improved on surfaces with lower values of the fractional polarity (FP), i.e. lower values of the polar components. The fractional polarity is defined as $\gamma_p / (\gamma_p + \gamma_d)$ and according to our calculations; the FP is reduced for the cpTi from 0.15 to 0.10, while for the SS increased from 0.12 to 0.19. Such an increment in combination with the larger positive charge on the surface might induce a detrimental response for the surface–biomolecule interactions.

Finally, the observation of the lower pzc of the cpTi (negatively charged surface at normal pH = 7.4) in comparison to the SS (positively charge), might help us to explain the major incorporation of Ca^{2+} ions on cpTi in comparison to SS, as has been shown by different authors for in-vivo and in-vitro experiments [77,78]. The electrostatic interaction between the cpTi-negatively charged surface and the positive ions leads to adsorption of Ca^{2+} ions which later make possible the subsequent adsorption of HPO_4^{2-} ions and the formation of a surface region

of calcium phosphate, which has been suggested to explain the osseointegration of titanium [77,79].

In summary, the exposure to 50 mM H_2O_2 solutions by 7 days induced stronger changes on the cpTi surface properties (roughness values, water contact angles, surface energy, point of zero charge and the impedance response) in comparison to the SS surface.

5. Conclusions

As a general conclusion, we observed that the simulated inflammation conditions lead to significant modifications in the surface properties of titanium and stainless steel substrates, such as the composition, roughness, surface energy and point of zero charge, although all the variations were larger on the Ti surfaces. The analysis of the electrochemical response indicated that the corrosion resistance of the Ti surface was decreased as a consequence of the interaction with the H_2O_2 rich solution, while not significant changes were observed for the SS. The higher dissolution/oxidation of the Ti surface induced the formation of a thicker surface oxide layer, which according to the impedance analysis showed a large porosity. The point of zero charge for the cpTi changes from 6.2 to 6.8, i.e. it became closer to neutral pH after the treatment and so, the amount of surface charge at this condition is reduced; leading to smaller electrostatic forces that could affect protein adsorption and conformation for in vivo response. The other significant variation after the H_2O_2 treatment, with consequence for the biological interactions of the material, was the decrease in the polar component of the surface energy for the cpTi, which has been associated to a better cellular adhesion and proliferation. Contrary, for the SS both the polar component and the pzc increased, indicating that at neutral pH, SS will be more positively charged. Therefore, the changes induced in the cpTi surfaces favored positively its biological response, contrary to the SS. The results from this work contributed to explain the better biological response of titanium surfaces when exposed to simulated inflammatory conditions in comparison to stainless steel.

Acknowledgements

The students (Fonseca-Garcia, Barrera and Medina) acknowledge support from CONACYT for the PhD scholarship. J. Pérez-Alvarez thanks DGAPA for the postdoctoral scholarship. Economical support to perform this research was provided by DGAPA-PAPIIT projects: PAPIIT IN118814, IN118914 and IG100113. Finally, we thank to C. Flores for helping us with the AFM characterization.

Appendix A. Supplementary data

Supplementary data to this article can be found online at http://dx.doi.org/10.1016/j.msec.2016.04.035.

References

[1] J.J. Ryu, P. Shrotriya, 2 - Synergistic mechanisms of bio-tribocorrosion in medical implants, in: Y. Yan (Ed.), Bio-tribocorrosion in Biomaterials and Medical Implants, Woodhead Publishing 2013, pp. 25–44.
[2] F. Variola, J.B. Brunski, G. Orsini, P.T. de Oliveira, R. Wazen, A. Nanci, Nanoscale surface modifications of medically relevant metals: state-of-the art and perspectives, Nanoscale 3 (2011) 335–353.
[3] P. Tengvall, I. Lundström, Physico-chemical considerations of titanium as a biomaterial, Clin. Mater. 9 (1992) 115–134.
[4] Y.T. Sul, B.S. Kang, C. Johansson, H.S. Um, C.J. Park, T. Albrektsson, The roles of surface chemistry and topography in the strength and rate of osseointegration of titanium implants in bone, J. Biomed. Mater. Res. A 89A (2009) 942–950.
[5] D.M.D. Ehrenfest, P.G. Coelho, B.S. Kang, Y.T. Sul, T. Albrektsson, Classification of osseointegrated implant surfaces: materials, chemistry and topography, Trends Biotechnol. 28 (2010) 198–206.
[6] R. Olivares-Navarrete, A.L. Raines, S.L. Hyzy, J.H. Park, D.L. Hutton, D.L. Cochran, B.D. Boyan, Z. Schwartz, Osteoblast maturation and new bone formation in response to titanium implant surface features are reduced with age, J. Bone Miner. Res. 27 (2012) 1773–1783.
[7] J. Pan, D. Thierry, C. Leygraf, Hydrogen peroxide toward enhanced oxide growth on titanium in PBS solution: blue coloration and clinical relevance, J. Biomed. Mater. Res. 30 (1996) 393–402.
[8] P. Tengvall, H. Elwing, L. Sjoqvist, I. Lundstrom, L.M. Bjursten, Interaction between hydrogen-peroxide and titanium — a possible role in the biocompatibility of titanium, Biomaterials 10 (1989) 118–120.
[9] C. Fonseca, M.A. Barbosa, Corrosion behaviour of titanium in biofluids containing H_2O_2 studied by electrochemical impedance spectroscopy, Corros. Sci. 43 (2001) 547–559.
[10] M. Karthega, S. Nagarajan, N. Rajendran, In vitro studies of hydrogen peroxide treated titanium for biomedical applications, Electrochim. Acta 55 (2010) 2201–2209.
[11] E. Unosson, K. Welch, C. Persson, H. Engqvist, Stability and prospect of UV/H_2O_2 activated titania films for biomedical use, Appl. Surf. Sci. 285 (2013) 317–323.
[12] E. Brooks, M. Tobias, K. Krautsak, M. Ehrensberger, The influence of cathodic polarization and simulated inflammation on titanium electrochemistry, J. Biomed. Mater. Res. B 102 (2014) 1445–1453.
[13] J.P. Bearinger, C.A. Orme, J.L. Gilbert, Effect of hydrogen peroxide on titanium surfaces: in situ imaging and step-polarization impedance spectroscopy of commercially pure titanium and titanium, 6-aluminum, 4-vanadium, J. Biomed. Mater. Res. A 67a (2003) 702–712.
[14] T. Albrektsson, P.I. Brånemark, H.-A. Hansson, B. Kasemo, K. Larsson, I. Lundström, D. McQueen, R. Skalak, The interface zone of inorganic implantsIn vivo: titanium implants in bone, Ann. Biomed. Eng. 11 (1983) 1–27.
[15] L.J.A. Heitz-Mayfield, A. Mombelli, The therapy of peri-implantitis: a systematic review, Int. J. Oral Maxillofac. Implants 29 (2014) 325–345.
[16] J. Pan, D. Thierry, C. Leygraf, Electrochemical and Xps studies of titanium for biomaterial applications with respect to the effect of hydrogen-peroxide, J. Biomed. Mater. Res. 28 (1994) 113–122.
[17] P. Tengvall, I. Lundstrom, L. Sjoqvist, H. Elwing, L.M. Bjursten, Titanium-hydrogen peroxide interaction — model studies of the influence of the inflammatory response on titanium implants, Biomaterials 10 (1989) 166–175.
[18] M. Morra, C. Cassinelli, Biomaterials surface characterization and modification, Int. J. Artif. Organs 29 (2006) 824–833.
[19] K.Y. Cai, J. Bossert, K.D. Jandt, Does the nanometre scale topography of titanium influence protein adsorption and cell proliferation? Colloid Surf., B 49 (2006) 136–144.
[20] C. Cassinelli, M. Morra, G. Bruzzone, A. Carpi, G. Di Santi, R. Giardino, M. Fini, Surface chemistry effects of topographic modification of titanium dental implant surfaces: 2. In vitro experiments, Int. J. Oral Maxillofac. Implants 18 (2003) 46–52.
[21] C. Galli, G.M. Macaluso, M. Piemontese, G. Passeri, Titanium topography controls FoxO/beta-catenin signaling, J. Dent. Res. 90 (2011) 360–364.
[22] G. Zhao, Z. Schwartz, M. Wieland, F. Rupp, J. Geis-Gerstorfer, D.L. Cochran, B.D. Boyan, High surface energy enhances cell response to titanium substrate microstructure, J. Biomed. Mater. Res. A 74A (2005) 49–58.
[23] P.M. Henson, The immunologic release of constituents from neutrophil leukocytes: II. Mechanisms of release during phagocytosis, and adherence to nonphagocytosable surfaces, J. Immunol. 107 (1971) 1547–1557.
[24] S.S. Kaplan, R.E. Basford, E. Mora, M.H. Jeong, R.L. Simmons, Biomaterial-induced alterations of neutrophil superoxide production, J. Biomed. Mater. Res. 26 (1992) 1039–1051.
[25] W.-W. Jiang, S.-H. Su, R.C. Eberhart, L. Tang, Phagocyte responses to degradable polymers, J. Biomed. Mater. Res. A 82A (2007) 492–497.
[26] D.W. Baker, J. Zhou, L. Tang, Chapter 14 — Methods used to evaluate the host responses to medical implants in vivo, in: S.F. Badylak (Ed.), Host Response to Biomaterials, Academic Press, Oxford 2015, pp. 425–440.
[27] M.I. Mokgobu, M.C. Cholo, R. Anderson, H.C. Steel, M.P. Motheo, T.N. Hlatshwayo, G.R. Tintinger, A.J. Theron, Oxidative induction of pro-inflammatory cytokine formation by human monocyte-derived macrophages following exposure to manganese in vitro, J. Immunotoxicol. 12 (2015) 98–103.
[28] W.F. Liu, M. Ma, K.M. Bratlie, T.T. Dang, R. Langer, D.G. Anderson, Real-time in vivo detection of biomaterial-induced reactive oxygen species, Biomaterials 32 (2011) 1796–1801.
[29] J.N. Israelachvili, 17 — Adhesion and wetting phenomena, in: J.N. Israelachvili (Ed.), Intermolecular and Surface Forces, third ed.Academic Press, San Diego 2011, pp. 415–467.
[30] F. Rupp, R.A. Gittens, L. Scheideler, A. Marmur, B.D. Boyan, Z. Schwartz, J. Geis-Gerstorfer, A review on the wettability of dental implant surfaces I: theoretical and experimental aspects, Acta Biomater. 10 (2014) 2894–2906.
[31] C.J. van Oss, Acid–base interfacial interactions in aqueous media, Colloids Surf. A Physicochem. Eng. Asp. 78 (1993) 1–49.
[32] C.J. Van Oss, R.J. Good, M.K. Chaudhury, The role of van der Waals forces and hydrogen bonds in "hydrophobic interactions" between biopolymers and low energy surfaces, J. Colloid Interface Sci. 111 (1986) 378–390.
[33] J.J. Gulicovski, L.S. Cerovic, S.K. Milonjin, Point of zero charge and isoelectric point of alumina, Mater. Manuf. Process. 23 (2008) 615–619.
[34] M. Kosmulski, Compilation of PZC and IEP of sparingly soluble metal oxides and hydroxides from literature, Adv. Colloid Interf. Sci. 152 (2009) 14–25.
[35] H. Shin, F. Mansfeld, Concerning the use of the Kramers–Kronig transforms for the validation of impedance data, Corros. Sci. 28 (1988) 933–938.
[36] B.S. Kang, Y.T. Sul, S.J. Oh, H.J. Lee, T. Albrektsson, XPS, AES and SEM analysis of recent dental implants, Acta Biomater. 5 (2009) 2222–2229.
[37] S. Giljean, M. Bigerelle, K. Anselme, Roughness statistical influence on cell adhesion using profilometry and multiscale analysis, Scanning 36 (2014) 2–10.
[38] R. Olivares-Navarrete, S. Hyzy, M. Berg, J. Schneider, K. Hotchkiss, Z. Schwartz, B. Boyan, Osteoblast lineage cells can discriminate microscale topographic features on titanium–aluminum–vanadium surfaces, Ann. Biomed. Eng. 42 (2014) 2551–2561.

[39] M. Bigerelle, P.E. Mazeran, W. Gong, S. Giljean, K. Anselme, A method to determine the spatial scale implicated in adhesion. Application on human cell adhesion on fractal isotropic rough surfaces, J. Adhes. 87 (2011) 644–670.
[40] J.M. Berg, L.G.T. Eriksson, P.M. Claesson, K.G.N. Borve, Three-component Langmuir–Blodgett films with a controllable degree of polarity, Langmuir 10 (1994) 1225–1234.
[41] E.A. Vogler, Protein adsorption in three dimensions, Biomaterials 33 (2012) 1201–1237.
[42] L. Ponsonnet, K. Reybier, N. Jaffrezic, V. Comte, C. Lagneau, M. Lissac, C. Martelet, Relationship between surface properties (roughness, wettability) of titanium and titanium alloys and cell behaviour, Mater. Sci. Eng. C 23 (2003) 551–560.
[43] T. Mekayarajjananonth, S. Winkler, Contact angle measurement on dental implant biomaterials, J. Oral Implantol. 25 (1999) 230–236.
[44] J.I. Rosales-Leal, M.A. Rodríguez-Valverde, G. Mazzaglia, P.J. Ramón-Torregrosa, L. Díaz-Rodríguez, O. García-Martínez, M. Vallecillo-Capilla, C. Ruiz, M.A. Cabrerizo-Vílchez, Effect of roughness, wettability and morphology of engineered titanium surfaces on osteoblast-like cell adhesion, Colloids Surf. A Physicochem. Eng. Asp. 365 (2010) 222–229.
[45] A. Mills, M. Crow, A Study of Factors that Change the Wettability of Titania Films, Int. J. Photoenergy 2008 (2008).
[46] J.H. Park, R. Olivares-Navarrete, R.E. Baier, A.E. Meyer, R. Tannenbaum, B.D. Boyan, Z. Schwartz, Effect of cleaning and sterilization on titanium implant surface properties and cellular response, Acta Biomater. 8 (2012) 1966–1975.
[47] R. Olivares-Navarrete, S.L. Hyzy, D.L. Hutton, C.P. Erdman, M. Wieland, B.D. Boyan, Z. Schwartz, Direct and indirect effects of microstructured titanium substrates on the induction of mesenchymal stem cell differentiation towards the osteoblast lineage, Biomaterials 31 (2010) 2728–2735.
[48] J.Y. Lim, M.C. Shaughnessy, Z. Zhou, H. Noh, E.A. Vogler, H.J. Donahue, Surface energy effects on osteoblast spatial growth and mineralization, Biomaterials 29 (2008) 1776–1784.
[49] N.P. Lang, G.E. Salvi, G. Huynh-Ba, S. Ivanovski, N. Donos, D.D. Bosshardt, Early osseointegration to hydrophilic and hydrophobic implant surfaces in humans, Clin. Oral Implants Res. 22 (2011) 349–356.
[50] K.L. Menzies, L. Jones, The impact of contact angle on the biocompatibility of biomaterials, Optom. Vis. Sci. 87 (2010) 387–399.
[51] B. Feng, J. Weng, B.C. Yang, J.Y. Chen, J.Z. Zhao, L. He, S.K. Qi, X.D. Zhang, Surface characterization of titanium and adsorption of bovine serum albumin, Mater. Charact. 49 (2002) 129–137.
[52] R.M. Salasznyk, W.A. Williams, A. Boskey, A. Batorsky, G.E. Plopper, Adhesion to vitronectin and collagen I promotes osteogenic differentiation of human mesenchymal stem cells, J. Biomed. Biotechnol. 2004 (2004) 24–34.
[53] Q. Huang, L. Lin, Y. Yang, R. Hu, E.A. Vogler, C. Lin, Role of trapped air in the formation of cell-and-protein micropatterns on superhydrophobic/superhydrophilic microtemplated surfaces, Biomaterials 33 (2012) 8213–8220.
[54] A. Wennerberg, R. Jimbo, S. Stübinger, M. Obrecht, M. Dard, S. Berner, Nanostructures and hydrophilicity influence osseointegration: a biomechanical study in the rabbit tibia, Clin. Oral Implants Res. 25 (2014) 1041–1050.
[55] P. Silva-Bermudez, S.E. Rodil, An overview of protein adsorption on metal oxide coatings for biomedical implants, Surf. Coat. Technol. 233 (2013) 147–158.
[56] A. Azioune, M.M. Chehimi, B. Miksa, T. Basinska, S. Slomkowski, Hydrophobic protein–polypyrrole interactions: the role of van der Waals and Lewis acid–base forces as determined by contact angle measurements, Langmuir 18 (2002) 1150–1156.
[57] M.N. Bellon-Fontaine, J. Rault, C.J. van Oss, Microbial adhesion to solvents: a novel method to determine the electron-donor/electron-acceptor or Lewis acid–base properties of microbial cells, Colloids Surf. B: Biointerfaces 7 (1996) 47–53.
[58] M. Musiani, M.E. Orazem, N. Pébère, B. Tribollet, V. Vivier, Constant-phase-element behavior caused by coupled resistivity and permittivity distributions in films, J. Electrochem. Soc. 158 (2011) C424–C428.
[59] M.E. Orazem, I. Frateur, B. Tribollet, V. Vivier, S. Marcelin, N. Pébère, A.L. Bunge, E.A. White, D.P. Riemer, M. Musiani, Dielectric properties of materials showing constant-phase-element (CPE) impedance response, J. Electrochem. Soc. 160 (2013) C215–C225.
[60] B. Hirschorn, M.E. Orazem, B. Tribollet, V. Vivier, I. Frateur, M. Musiani, Constant-phase-element behavior caused by resistivity distributions in films: II. Applications, J. Electrochem. Soc. 157 (2010) C458–C463.
[61] M. Aziz-Kerrzo, K.G. Conroy, A.M. Fenelon, S.T. Farrell, C.B. Breslin, Electrochemical studies on the stability and corrosion resistance of titanium-based implant materials, Biomaterials 22 (2001) 1531–1539.
[62] J.E.G. Gonzalez, J.C. Mirza-Rosca, Study of the corrosion behavior of titanium and some of its alloys for biomedical and dental implant applications, J. Electroanal. Chem. 471 (1999) 109–115.
[63] L.P. Faverani, V.A.R. Barão, G. Ramalho-Ferreira, M.B. Ferreira, I.R. Garcia-Júnior, W.G. Assunção, Effect of bleaching agents and soft drink on titanium surface topography, J. Biomed. Mater. Res. B Appl. Biomater. 102 (2014) 22–30.
[64] U. Rammelt, G. Reinhard, The influence of surface roughness on the impedance data for iron electrodes in acid solutions, Corros. Sci. 27 (1987) 373–382.
[65] M. Gasik, A. Braem, A. Chaudhari, J. Duyck, J. Vleugels, Titanium implants with modified surfaces: meta-analysis of in vivo osteointegration, Mater. Sci. Eng. C 49 (2015) 152–158.
[66] S. Abey, M.T. Mathew, D.J. Lee, K.L. Knoernschild, M.A. Wimmer, C. Sukotjo, Electrochemical behavior of titanium in artificial saliva: influence of pH, J. Oral Implantol. 40 (2014) 3–10.
[67] J.M. Anderson, A. Rodriguez, D.T. Chang, Foreign body reaction to biomaterials, Semin. Immunol. 20 (2008) 86–100.
[68] K.S. Jones, Effects of biomaterial-induced inflammation on fibrosis and rejection, Semin. Immunol. 20 (2008) 130–136.
[69] W.-J. Hu, J.W. Eaton, T.P. Ugarova, L. Tang, Molecular basis of biomaterial-mediated foreign body reactions, Blood 98 (2001) 1231–1238.
[70] B. Beutler, Innate immunity: an overview, Mol. Immunol. 40 (2004) 845–859.
[71] C. Wittmann, P. Chockley, S.K. Singh, L. Pase, G.J. Lieschke, C. Grabher, Hydrogen peroxide in inflammation: messenger, guide, and assassin, Adv. Hematol. 2012 (2012) 6.
[72] S.E. Headland, L.V. Norling, The resolution of inflammation: principles and challenges, Semin. Immunol. 27 (2015) 149–160.
[73] X. Zhidao, T.T. James, A review on macrophage responses to biomaterials, Biomed. Mater. 1 (2006) R1.
[74] K.V. Eaton, H.L. Yang, C.M. Giachelli, M. Scatena, Engineering macrophages to control the inflammatory response and angiogenesis, Exp. Cell Res. 339 (2015) 300–309.
[75] J.S. Hayes, E.M. Czekanska, R.G. Richards, The cell-surface interaction, Adv. Biochem. Eng. Biotechnol. 126 (2012) 1–31.
[76] S. Genet, R. Costalat, J. Burger, A few comments on electrostatic interactions in cell physiology, Acta Biotheor. 48 (2000) 273–287.
[77] T. Hanawa, M. Ota, Calcium-phosphate naturally formed on titanium in electrolyte solution, Biomaterials 12 (1991) 767–774.
[78] B. Kasemo, Biocompatibility of titanium implants: surface science aspects, J. Prosthet. Dent. 49 (1983) 832–837.
[79] T. Hanawa, M. Ota, Characterization of surface-film formed on titanium in electrolyte using Xps, Appl. Surf. Sci. 55 (1992) 269–276.